The complexity of event-related MEG signals decreases with maturation in human fetuses and newborns

Joel Frohlich[1], Julia Moser[2,3], Pedro A. M. Mediano[4,5], Hubert Preissl[2†], Alireza Gharabaghi[1†]

[1]Institute for Neuromodulation and Neurotechnology, University Hospital and University of Tübingen, Germany
[2]IDM/fMEG Center of the Helmholtz Center Munich at the University of Tübingen, University of Tübingen, German Center for Diabetes Research (DZD e.V.), Tübingen, Germany
[3]Masonic Institute for the Developing Brain, University of Minnesota, Minneapolis, MN, USA
[4]Department of Computing, Imperial College London, London, UK
[5]Department of Psychology, University of Cambridge, Cambridge, UK

†These authors contributed equally (senior coauthorship)

Running title: Perinatal cortical entropy

Abstract: 150 words

Introduction: 901 words

Results: 2188 words

Discussion: 1814 words

Materials and Methods: 3634 words

Main manuscript: 4903 (without Methods), 8537 words (with Methods)

References: 80

Display items: 6 Figures and 4 Tables

Abstract

It is unknown how cortical entropy or “complexity”, a marker of consciousness, evolves in early human development. To test the hypothesis that the entropy of cortical signals increases approaching birth, we conducted the first ever study to relate fetal cortical entropy to maturation. MEG recordings were obtained from a sample of fetuses and newborns with prior evidence of perceptual consciousness. Using cortical responses to auditory irregularities, we computed several measures of signal entropy. Despite our hypothesis, cortical entropy significantly decreased with maturation in fetuses and newborns, with the strongest effect occurring with 4 – 10 Hz permutation entropy in both groups. Decreases in permutation entropy were driven by amplitude changes in both fetuses and newborns, whereas phase and its interaction with amplitude drove increases in entropy, possibly related to consciousness. These results lay groundwork both for future measures of perinatal consciousness and new in utero estimates of risk for neurodevelopmental disorders.

Teaser: Even as birth nears, a neural marker of consciousness decreases with gestational age in late fetal development and continues to decline after birth.

Keywords: Fetus; infant; MEG; complexity; entropy; neurodevelopment; consciousness

Introduction

The complexity of cortical signals is captured by entropy, or the number of unique ways in which states of a signal can be arranged. Entropy has been successfully used as a proxy for the level of consciousness across a wide range of conditions and populations (*1*). In adults, it decreases relative to wakefulness as consciousness vanishes in non-rapid eye movement (NREM) sleep (*2*, *3*), anesthesia (*4*, *5*), and disorders of consciousness such as the coma and vegetative state (*2*, *6*), and it increases as phenomenology gains vividness and intensity during hallucinatory states induced by psychedelic substances relative to ordinary wakefulness (*7*, *8*) and lucid dreaming relative to non-lucid dreaming (*9*). Similarly, in both neurotypical children and children with abnormal cortical dynamics linked to genetic disorders, cortical entropy also tracks diminished consciousness during NREM sleep and outperforms spectral markers as an indicator of consciousness (*10*).

In a broader context, neural complexity often positively reflects cortical health, as demonstrated in Alzheimer's disease (*11*, *12*), cognitive aging (*13*), autism spectrum disorder (ASD) (*14–16*), and attention deficit hyperactivity disorder (*17*, *18*). While neural complexity shows an inverse relationship with these conditions (i.e., complexity is considered healthy), in other instances, excessive complexity may reflect disorganized neural firing patterns or excessive flexibility of circuits, e.g., in schizophrenia (*19*, *20*). These lines of evidence, combined with analogous findings from other organ systems (*21–23*), suggest that optimal levels of physiological complexity might be general signatures of adaptability, flexibility, and fitness (*24*).

Given the foregoing, neural complexity should be expected to track both healthy neurodevelopment and the emergence of consciousness in the earliest stages of life. Along these lines, two early electroencephalography (EEG) studies of infancy found differences in signal complexity (measured as dimensionality) between sleep stages (suggesting differences in conscious level), as well as higher complexity in full-term infants compared with preterm infants who had reached the same postmenstrual age (*25*, *26*) (suggesting differences in cortical development). A later study reproduced this finding using different complexity measures and also found evidence that skin-to-skin care between mothers and preterm infants restores neural complexity in a small cohort (*27*). Another study that examined a similar intervention with a larger sample size (*28*) tested the integrated information theory (IIT) of consciousness (*29*) by estimating EEG complexity in preterm infants as integrated information. The authors found that this measure relates to conscious state and increases with postmenstrual age in preterm infants; moreover, the latter relationship shows a steeper slope for preterm infants who receive greater maternal care (*28*).

Beyond infancy, it is known that cortical signal complexity increases with age in early (*30*, *31*) and late (*32*, *33*) childhood, yet the picture prior to birth has remained terra incognita. While a proof-of-principle study has demonstrated that the signal-to-noise ratio (SNR) of fetal

magnetoencephalography recordings (generally referred to as fMEG) is sufficient to meaningfully compute cortical complexity measures (*34*), the extent to which such measures track brain development, maturation, cortical health, or the capacity for consciousness in fetuses remains unknown.

In this study, we measured cortical responses to auditory irregularities with MEG recordings that passed rigorous quality control in a sample of fetuses and newborns for whom evidence of perceptual consciousness has already been inferred in prior work using a local-global paradigm (*35*, *36*). This paradigm, which measures cortical responses to sensory irregularities (or "oddballs") in a hierarchical learning context, has been previously used to infer consciousness in adult neurological patients (*37*–*39*). Because oddballs generate a Bayesian prediction error, we reasoned that they should more strongly perturb the thalamocortical system than repetitive trains of identical stimuli. Our approach thus takes inspiration from the perturbation complexity index (PCI) of consciousness (*2*), which emphasizes causal influences within a system (*29*). We therefore computed entropy from event-related data in contrast to the spontaneous entropy approaches cited earlier (*25*–*28*) and utilized two different auditory sequences (with and without local deviant tones). We hypothesized that cortical entropy would increase with maturation in fetuses as consciousness develops approaching birth, and also in newborns, as consciousness further develops in early infancy. Additionally, because fetal behavioral states are categorized in large part using heart rate variability (HRV) (*40*), we also hypothesized that cortical entropy would increase with HRV, as more active fetuses might plausibly be in a more conscious state compared with inactive or sleeping fetuses.

To test these hypotheses, we utilized several distinct entropy measures, as well as decompositions of the MEG signal into amplitude and phase components and comparisons of the MEG signal entropy to that of surrogate signals. Finally, to better understand the relationship between entropy and oscillations, we also correlated entropy with spectral power and examined event related spectral perturbations (ERSPs) in relation to maturation and arousal. Our results for the total entropy change and amplitude component, which contradict our hypothesis, are perhaps the first observation of brain dynamics descending from a state of high entropy as the brain's capacity for consciousness increases, rather than decreases. Our results for the non-amplitude component of the permutation entropy change, on the other hand, demonstrate increasing entropy with age, as we originally hypothesized, perhaps related to an increasing capacity for consciousness. By exploring the behavior of entropy in response to auditory irregularities in fetuses and newborns, our results may pave the way for both biomarkers of perinatal consciousness analogous to the PCI (*41*) and in utero detection of neurodevelopmental disorder risk as indicated by abnormal cortical entropy trajectories.

Results

We utilized data that were collected from a previous study at the fMEG Center at the University of Tübingen. Recorded signals included both cortical activity (MEG) and cardiac activity (magnetocardiography or MCG), the latter of which was retained to measure HRV (one of the main parameters used to classify fetal behavioral and sleep states (*40*)) and, by proxy, arousal. The dataset consisted of 81 usable recordings of cortical and cardiac signals from 43 fetuses (gestational age range: 25 – 40 weeks) which passed strict MEG quality control. Of these data, 75 recordings from 41 fetuses also contained usable MCG data; thus, only these data were used in the main analyses of fetal data that included HRV as a predictor. Two additional recordings lacking usable cardiac data were utilized in a follow up analysis (see "Maturation diminishes entropy through changes in MEG signal amplitude" below). For a description of which data were used in which analyses, see Tables S1 and S2. We additionally included 20 recordings from 20 newborns (age range: 13 – 59 days) acquired with the same MEG system and which also passed strict MEG quality control. Each experiment exposed fetuses and newborns to two blocks of stimuli: sequences of identical tones ('ssss') or nonidentical tones ('sssd'). In a subsequent test phase, sequences occasionally violated the block rule (capital letters denote rule violations). See Methods and Materials for additional details.

We computed the signal entropy on the MEG signals averaged across trials and channels (see Materials and Methods), according to six approaches. Two approaches, Lempel-Ziv complexity (LZC) and context tree weighting (CTW), measure the compressibility of the signal. The remaining approaches are based on state-space reconstruction of the signal and include modified sample entropy (mSampEn, or the tendency of motifs to reoccur within a signal), modified multiscale entropy (mMSE, which computes mSampEn at different time scales), and permutation entropy (PermEn, or the occurrence of unique permutations based on ordinal rankings of data). We computed two different varieties of PermEn using a 32 ms lag (PermEn32, sensitive to 4 – 10 Hz activity) and a 64 ms lag (PermEn64, sensitive to 2 – 5 Hz activity). To account for longitudinal fetal data, we computed correlations from fetal data using normalized β regression coefficients. We corrected for multiple comparisons using the Benjamini-Hochberg (*42*) false discovery rate (FDR). For ERSPs, we also corrected for multiple comparisons using permutation cluster statistics before applying the FDR correction.

Cortical entropy declines with maturation in fetuses and newborns

In fetuses, all six entropy measures significantly decreased with maturation (Fig. 1, Table 1). The largest such effect was observed for PermEn32, which is sensitive to activity in the 4 – 10 Hz range ($t = -4.71$, $P_{FDR} < 0.0001$). PermEn64, which is sensitive to activity in the 2 – 5 Hz range, showed only a marginally significant negative relationship with gestational age ($t = -2.57$, $P_{FDR} = 0.03$). Thus, the largest fetal cortical entropy changes with maturation appear localized to the 4 – 10 Hz band, which may encompass the alpha band in early development (*43*). In newborns, as in

fetuses, PermEn32 showed the strongest relationship with maturation, significantly decreasing with age ($t = -3.85$, $P_{FDR} < 0.005$); note that this relationship was only cross-sectional, as no longitudinal data were obtained from newborns. The same relationship was not significant in newborns for PermEn64 ($t = -1.61$, $p > 0.05$) suggesting, again, that entropy changes are mainly localized to the 4 – 10 Hz band measured with PermEn32. Two other entropy measures, CTW ($t = -2.45$, $p = 0.05$) and mSampEn ($t = -2.72$, $p = 0.03$), were marginally significant in newborns, also showing negative correlations with age. The remaining entropy measures did not significantly relate to maturation in newborns but nonetheless showed the same directionality as other measures, i.e., a negative relationship with age. See Table 1 for exact P-values. Arousal (inferred from HRV) did not significantly predict changes in any entropy measures for either group.

Because fetal data contained multiple recordings from some subjects, we next evaluated whether these recordings could be approximated as independent samples by examining the usefulness of the random intercept term in the fetal LMMs. For each fetal model except for the LMM predicting PermEn64, the random effect term significantly increased the model fit ($P < 10^{-6}$, log-likelihood ratio test, uncorrected, Table S3), implying substantial dependencies between longitudinal recordings from the same subjects with consequences for our correlational analyses (see Fig. S3).

After running linear mixed models (LMMs), we next computed correlations between entropy measures and maturation in fetuses and newborns (Fig. 1). These post hoc tests revealed a numeric pattern of stronger correlations for the global deviant sssD in both fetuses and for the global deviant sssS in newborns. Many correlations between age and entropy measures derived from newborns were moderate in degree with the same sign (negative) as those seen in fetuses [$r < -0.3$, 13/24 (54%)]. For comparison, this proportion was smaller in the fetal correlations [derived from model coefficients, $\beta < -0.3$, 8/24 (33%)]; thus, we may have been underpowered to detect a significant finding in some entropy measures (LZC, mMSE, and PermEn64) due to our small neonatal sample. Positive correlations between entropy and maturation were rare, occurring exclusively in the sssd condition in newborns (see Fig. 1).

Changes in MEG signal amplitude drive maturational decreases in signal entropy

To determine whether the decline in entropy with maturation was driven by changes in the MEG signal amplitude (e.g., the maturation of ERF component amplitudes) or by non-amplitude changes (i.e., changes in the MEG signal phase and its interaction with amplitude), we performed an entropy decomposition (*44*), which entailed randomizing Fourier phases to isolate the contributions of amplitude, phase, and their interaction (see Materials and Methods). In fetal MEG recordings, we performed this analysis using only those fetuses with longitudinal data from both early and late gestation, defined as before and after the 35 week mark. We further restricted

this analysis to the sssD condition, which had yielded the strongest relationship between entropy and gestational age in fetuses (Fig. 1). We identified n = 12 fetuses with data from both prior to 35 weeks gestational age ("early") and 35 weeks or later ("late"), choosing 35 weeks as the threshold based on evidence from a prior study that fetuses begin to show cortical responses to deviant tones at this gestational age (*35*). In cases where fetuses meeting this criterion had more than two recordings, we used the earliest recording for the early condition and the latest recording for the late condition. Note that two fetal recording from separate participants that were excluded from other analyses due to missing HRV data were included here (Table S1). In neonatal MEG recordings, we applied a median split at an age of 33 days in participants with usable data (n = 18) in the sssS condition (i.e., the data that yielded the strongest post hoc correlations between entropy and age in newborns). This allowed us to compare entropy changes between 9 younger and 9 older newborns using the same entropy decomposition that was applied to fetal data. Because we lacked longitudinal data in the neonatal cohort and thus could not examine entropy changes using a paired-samples approach, we computed differences using all possible pairings between age groups (see Materials and Methods). For each neonatal recording, we then computed the average difference between its entropy and the entropy of the neonatal recordings in the other age group. Next, we compared these average differences between amplitude and non-amplitude contributions. Because our findings were identical regardless of whether this contrast was performed referenced to the younger versus the older subgroup of newborns, we arbitrarily chose the younger subgroup for reporting our results below; results referenced to the older subgroup are reported in Table S4.

We discovered that, for both measures of PermEn (i.e., PermEn32, sensitive to 4 – 10 Hz activity, and PermEn64, sensitive to 2 – 5 Hz activity), amplitude and non-amplitude properties of the signal caused opposite changes between early and late timepoints in both fetuses and newborns (Fig. 2). Specifically, as seen in Fig. 2 for both fetal and neonatal data, the MEG signal amplitude was responsible for the decline in entropy (i.e, ΔPermEn < 0, old - young), whereas the non-amplitude properties (phase and phase x amplitude interactions) drove changes in the opposite direction (i.e, ΔPermEn > 0, old - young). The difference between amplitude and non-amplitude contributions was highly significant (Table 2) for both PermEn32 and PermEn64 in fetuses and newborns ($P_{FDR} < 10^{-10}$). Although the magnitude of these changes were similar between amplitude and non-amplitude components (Fig. 2), the absolute value of the amplitude component was larger in all cases except PermEn64 in newborns, resulting in larger PermEn at earlier timepoints in those cases where LMMs had already revealed statistically significant entropy decreases with age. Thus, PermEn ultimately declines with maturation in fetuses and newborns due to MEG signal amplitude, despite the opposing influence of non-amplitude factors. Other entropy measures did not yield significant differences in changes attributable to amplitude versus non-amplitude components in fetuses or newborns (Fig. S1). Note that we obtained the same results when entropy differences were references to older newborns (Fig. S2).

Evidence of cortical stochasticity in fetuses and neonates

To assess the degree to which cortical MEG signals differed from noise, i.e., surrogate signals with the same amplitude distribution, we next tested whether the entropy estimates for cortical signals were significantly different from the entropy of surrogates. No entropy measures significantly distinguished cortical signals from surrogates (Table 3). This null result suggests that MEG signals lack nonlinear components that affect entropy. Given this likely lack of nonlinearity, at least some degree of stochasticity, or intrinsic randomness, appears to be present in MEG signals. Using the Toker decision tree algorithm (*45*), we found that the proportion of signals with deterministic dynamics was significantly larger in fetuses than in newborns (χ^2 = 30.8, P = 2.8 x 10^{-8}, uncorrected; note that each recording was treated as an independent sample), yet neither maturation nor arousal predicted signal dynamics in fetuses or newborns (Fig 3, Table S5).

Entropy measures correlate strongly with one another and weakly with spectral power

To better understand the behavior of cortical entropy measures in our data, we computed correlations between these measures. As expected, in both fetal and neonatal data, entropy measures were positively correlated with one another (Fig. 4A,B), many strongly so (fetal range: β = 0.42 – 0.97; neonatal range: r = 0.61 – 0.97), showing these measures are approximately capturing a reliable underlying property of the MEG signal. Although we used beta coefficients to measure correlations in fetal data with longitudinal recordings, beta coefficients returned very similar values as Pearson coefficient (Fig. S3). Next, we examined correlations between signal complexity measures and spectral power. Entropy measures were negatively correlated with spectral power at all frequencies in newborns (range: r = -0.77 – -0.089) and at frequencies < 5.5 Hz in fetuses (range: β =-0.48 – -0.09), demonstrating that cortical synchronization introduces regularities into cortical signals that constrain their entropy (Fig. 4C,D). However, this relationship between entropy and power reversed at faster frequencies in fetuses, with moderate correlations as high as β = 0.36 for power at 9.5 Hz. Finally, we utilized time-resolved CTW to evaluate the relationship between entropy and spectral power within each recording. This within-recording analysis was only performed using CTW, given its high temporal resolution; we accepted this analysis as being representative of entropy in general, given that CTW is highly correlated with other entropy measures. We found that, after averaging TFRs and time-resolved CTW across all datasets, CTW was not strongly correlated with spectral power at most frequencies in fetuses and newborns; note that correlation coefficients were averaged in a nested fashion (first with-subjects, then between-subjects) to ensure that subjects with longitudinal data were not overrepresented. After averaging correlation coefficients across all four stimulus x block rule combinations, we found that the absolute value of the mean correlation did not exceed 0.25 for any frequency in fetal or neonatal data (Fig. 4E,F). Thus, signal entropy appears to be weakly correlated with spectral power within each dataset, but negatively—and, in some cases, strongly—correlated with spectral power between datasets.

Cortical synchronization increases with maturation in fetuses and newborns

Finally, we examined how maturational variables influenced ERSPs in fetal and neonatal data. Using permutation cluster statistics, we observed three significant clusters (AGE term in model, $P_{FDR} < 0.005$) in time-frequency representations from fetal data in which more mature fetuses demonstrated greater synchronization (Fig. 5A,B, Table 4), with this effect occurring within the delta frequency range (1 – 3 Hz). In newborns, we observed broadband synchronization with increasing maturation in ERSPs, yielding eight significant clusters ($P_{FDR} < 0.005$) for the AGE term in our model (Fig. 5C,D, Table 4). Newborns also yielded three significant clusters ($P_{FDR} < 0.005$) for the HRV model term, showing greater power with lower arousal at low frequencies corresponding to delta or theta (Fig. 5E,F, Table 4). For a full description of all time-frequency clusters with exact P-values, including those that were not statistically significant, see Table 4. For TFRs of trial-averaged ERFs in each condition, see Fig. S4.

Discussion

In this study, we tested the hypothesis that fetal cortical entropy increases as the brain's capacity for consciousness increases approaching birth, and that this trajectory continues after birth in newborns. Importantly, we utilized a sample of fetuses and newborns with prior evidence of perceptual consciousness (*35*). Although we built on a proof-of-concept study (*34*), our current work is the first to test hypotheses that these entropy measures change with physiological variables such as age and arousal in fetuses.

Despite our expectation that cortical entropy would increase with maturation, we were surprised to discover significant decreases in total entropy in all measures of cortical signal complexity in fetuses and several measures in newborns. In both fetuses and newborns, the strongest effect of maturation was obtained using PermEn32, which is maximally sensitive to activity in the 4 – 10 Hz range, i.e., the perinatal alpha band (*43*). However, an entropy decomposition revealed that these changes are specifically driven by changes in signal amplitude with maturation, whereas other signal changes—possibly related to the emergence of consciousness—drive increases in PermEn. Thus, the total effect of decreasing entropy with perinatal maturation may actually be the net result of two separate maturational processes with opposite effects on PermEn, although evidence for this was not observed using other entropy measures.

While fewer entropy measures significantly related to maturation in newborns as in fetuses, many correlations between age and entropy in newborns were in fact of larger magnitude than those measured in fetuses and shared the same direction (negative). This could potentially be explained by the fact that we may have been underpowered to predict some entropy measures from age in our small sample of newborns (N = 20). Alternatively, we may have had fewer findings in newborns because the cradle is a less controlled environment than the womb (*41*).

Toward an index of perinatal consciousness

Cortical entropy is typically measured either from spontaneous EEG or MEG signals (*5*, *7*), or using cortical responses to perturbations (*2*), recorded with EEG, to noninvasive transcranial magnetic stimulation (TMS). The latter approach, known as the PCI (*2*), is inspired by IIT, which emphasizes the role of casual influences within a system as the basis of consciousness (*29*). Despite its excellent empirical performance discriminating states of consciousness in adults (*6*), PCI's application excludes fetuses and infants for whom the developmental risks of TMS are not fully understood. A safer alternative, however, is offered by sensory stimulation, which also perturbs the cortex, albeit in a very different fashion (*46*). These sensory perturbations may be useful for inferring the developmental onset of conscious awareness (*41*).

Our application of entropy measures to cortical signals resulting from auditory prediction errors in fetuses and newborns is inspired by, yet different from, PCI based on TMS-perturbations in adults (*6*). Although we are hopeful that a sensory PCI might be achievable in the near future;

[for a discussion of feasibility, see Frohlich et al. (*41*)], we caution that, unlike published PCI algorithms, our calculations of cortical entropy measures in the present study did not take into account spatial entropy, as we averaged signals across 5 (newborns) or 10 (fetuses) MEG channels to overcome SNR limitations in our noisy recordings. This might explain why the total cortical entropy decreased with maturation in fetuses and newborns, despite a reasonable expectation that the brain's capacity for conscious experience (which relates positively to cortical entropy) will increase, rather than decrease, over this time period. Had our SNR been sufficient to forego channel-averaging and instead compute the full spatiotemporal entropy pattern, it is plausible that the decrease in temporal entropy that occurs in fetal signals with maturation would have been counter-balanced or exceeded by an increase in spatial entropy over the same developmental period (Fig. 6B). This explanation is supported by the fact that corticocortical connectivity, whose measurement requires resolving the activity of spatially distributed sensors, is responsible for decreases in PCI during unconsciousness (*47*). On the other hand, the P300 response elicited by sensory oddballs is longer and less spatially varied (*48*) compared with TMS-evoked potentials (*49*), suggesting than entropy could still decrease with maturation even when a full temporospatial pattern is accounted for.

Causes of cortical entropy changes in late fetal developmental

Considering non-amplitude effects on PermEn, our original hypothesis that perinatal increases in the capacity for consciousness should manifest as increases in cortical entropy may still be partially correct though not reflected in the total entropy change. The maturation of ERF components, which introduce structure into cortical signals, thereby constraining their entropy (Fig. 6A), may mask the hypothesized increase. This interpretation is supported by the fact that signal amplitude is responsible for the decrease in PermEn (Fig. 2). Previous work in the same sample of fetuses has shown maturation of P300-like cortical responses to deviant tones late in the third trimester, with fetuses demonstrating stronger responses past 35 weeks gestation as compared to younger fetuses (*35*). However, in later development (one month to adulthood), the entropy of event-related cortical signals increases even as the responses mature and grow in amplitude (*31*, *32*). Thus, it seems that entropy relates negatively with amplitude during the perinatal period, but this relationship may reverse in later development.

Alternatively, one may also view the decrease in fetal cortical entropy with maturation through the lens of the entropic brain hypothesis (EBH) (*50*, *51*). EBH emphasizes the entropy of spontaneous, rather than perturbed, brain activity as an index of the informational and phenomenological richness of conscious states. Although this relationship is generally positive in adults (*3*, *5*, *7*, *8*) and young children (*10*, *52*), one prediction of EBH is that the richness of conscious content should diminish if entropy exceeds a "critical zone" that is optimal for consciousness and information processing (*50*). One may therefore speculate that in perinatal development, the cortex begins in an over-entropic state, and that cortical entropy must decrease (e.g., via sculpting processes such as apoptosis and synaptic pruning) (*53*) before

consciousness emerges. However, this interpretation would also predict that cortical signals change their dynamics as the cortex descends into a critical state. Contrary to this prediction, signal dynamics were not significantly associated with maturation in data from fetuses or newborns (Fig. 3, Table S5).

Fetal cortical entropy as an indicator of circuit flexibility and neurodevelopmental trajectories

Above, we have assumed cortical entropy should track consciousness during perinatal development. Alternatively, however, changes in the total cortical entropy may reflect a different construct, such as the flexibility of cortical circuits. This view is supported by the fact that we failed to find a relationship between arousal (measured as HRV) and entropy (Table 1), even though these two variables are tightly related in most contexts (*54*, *55*) and, moreover, that the relationship we did detect between maturational changes and total entropy changes showed the opposite direction (Fig. 1) as what one would likely hypothesize, given that entropy is a marker of consciousness (*1*).

If the total cortical entropy measured from event-related perinatal MEG signals does not reflect the level of consciousness, an alternative interpretation of the cortical entropy changes we detected is that they relate to the evolving flexibility and adaptability of cortical circuits. Indeed, neural entropy has been previously described in this context (*24*), possibly explaining its reduction in many brain disorders and disease states (*11*–*13*, *17*, *18*, *16*). Nonetheless, excessive neural entropy may reflect excessive flexibility whereby circuits fail to function properly, e.g., in schizophrenia (*19*, *20*). Similarly, neural entropy might also indicate the progress of developmental forces. In ontogenesis, neural circuits may begin in many different patterns (high entropy) but converge toward a “canal” or mature pattern of activity (low entropy) through developmental processes such as apoptosis and synaptic pruning (Fig. 6D) (*53*).

Because this process continues after birth, neural entropy has been used to track abnormal neural development and predict an eventual diagnosis of the neurodevelopmental disorder autism from EEG recorded as early as 3 months of age (*14*). Our finding that neural entropy decreases with gestational age might allow for new techniques that uses fetal entropy trajectories to assess the risk for neurodevelopmental disorders which largely begin in utero, including ASD and schizophrenia (*56*–*58*). The etiology of both disorders is thought to involve aberrant or excessive synaptic pruning (*59*, *60*), which may be preceded by abnormal circuit development in utero. Given that entropy features derived from infant EEG recordings have recently shown promise for assessing ASD risk (*14*, *15*), fetal MEG signal entropy changes, influenced by circuit maturation (Fig. 6D), might be used to detect a developing fetus’s risk of neurodevelopmental disorders later in life. A predictive biomarker such as this is greatly needed to initiate early interventions (*61*).

Limitations, future directions, and conclusions

Herein, we have presented the first ever evidence of evolving cortical entropy during late fetal development. Combined with cross-sectional evidence from newborns, these results suggest a continuous decline in cortical entropy from late gestation to several weeks after birth. Our findings are admittedly limited by the low SNR of our recordings, which precluded our ability to study spatial changes in entropy with maturation or to examine oscillations in the beta and gamma range. Furthermore, our efforts to explore cortical entropy as a perinatal marker of consciousness are arguably limited by the inaccessibility of a ground truth, whereby we may only trust such markers insofar as they relate to consciousness in adults and children. Finally, even if neural markers of consciousness in adults carry the same meaning in fetuses and newborns, it remains uncertain whether sensory perturbations can be used in the same manner as TMS perturbations for detecting consciousness. For a detailed discussion of these final two issues, see Frohlich et al. 2022 (*41*).

A notable strength of our study was the inclusion of a large sample of fetuses with both cross-sectional and longitudinal sampling to study development. Although MEG signals from newborns—which we also recorded—offer a better SNR, fetal data offer the advantage that the womb is a highly controlled environment that regulates fetal arousal and isolates the fetus from many environmental distractors (*41*). Furthermore, our study was strengthened by the inclusion of fetal and neonatal cohorts for whom evidence of perceptual consciousness had already been established (*35*, *36*).

In conclusion, a key finding of our study is a realtionship between perinatal cortical entropu and maturation which suggests that entropy tracks an important developmental process in utero. Our work builds on an earlier proof-of-concept study (*34*) to demonstrate the successful application of entropy measures to fetal MEG signals and lays the groundwork for both for in utero assessments of ASD and schizophrenia risk and for quantitative inferences of conscious level in fetuses and newborns (e.g., using “sensory PCI”). Future investigations, particularly using optically pumped magnetometers to record MEG (*62*–*64*), should map spatial changes in perinatal cortical entropy and further investigate the feasibility of a PCI-like index of perinatal consciousness using sensory perturbations.

Materials and Methods

Study population

This work utilized publicly available (fetal data: https://zenodo.org/record/4541463#.Y0a-iExByHt; neonatal data: https://zenodo.org/record/4018827#.Y0a-akxByHt) which were acquired for and previously analyzed in studies of hierarchical learning in fetuses (*35*) and newborns (*36*) that revealed markers of perceptual consciousness in both cohorts. Previous studies from which the data were obtained recruited parents or mothers-to-be who volunteered data from their newborn infants (N = 33) or fetuses (N = 60), respectively. Some mothers-to-be gave fetal data at multiple visits (see below). Newborns were 13 – 59 days old at the time of MEG recording. The study was approved by the local ethics committee of the Medical Faculty of the University of Tübingen. Consent to participate in the experiment was signed by the mother-to-be (fetal group) or both parents (neonatal group).

MEG recordings

Fetal and neonatal cortical signals were recorded in the context of earlier studies (see above) using the SARA (SQUID array for reproductive assessment, VSM MedTech Ltd., Port Coquitlam, Canada) system in a magnetically shielded room (Vakuumschmelze, Hanau, Germany) at the fMEG Center at the University of Tübingen. The SARA system is an MEG machine built for recording fetal data, with SQUID (superconducting quantum interference device) sensors arranged in a concavity that fits the maternal abdomen. All MEG signals were sampled at 610.3516 Hz; this legacy sampling rate originates from the need to avoid interference from other radio signals during system installation. Recorded signals included both cortical activity (MEG) and cardiac activity (MCG), the latter of which was retained to measure HRV and arousal. Fetal head position was determined before and after each MEG recording using ultrasound (Ultrasound Logiq 500MD, GE, UK), and the first measurement was used to place a positioning coil on the maternal abdomen. Three additional positioning coils were placed around the abdomen (left and right sides, and one on the spine) to track changes in the position of the mother-to-be's body. Recordings with excessive positional changes were discarded. The SARA system was also used to record neonatal cortical signals by placing newborns in a crib resting head-first toward the sensor array. All newborns were positioned lying on their left side, such that auditory stimuli could be delivered to the right ear. The SARA system is completely noninvasive and utilizes 156 primary sensors and 29 reference sensors. Because the sensor array, built to compliment the maternal abdomen, is much larger than the fetal or neonatal head, in both cases cortical signals are received largely by a subset of sensors that are located near the head.

Experiments

Experiments with fetuses and newborns used a local-global paradigm with pure tones (200 ms each) of two frequencies, 500 and 750 Hz. For each participant, one frequency was assigned as a standard tone and the other as a deviant tone. Assignments were kept consistent for participants with longitudinal visits, but varied randomly across different participants. Each experiment consisted of two blocks in randomized order, counter-balanced across participants: in one block, fetuses and newborns were trained with 30 sequences each consisting of either four identical standard tones (block rule: 'ssss') or three identical standard tones followed by a deviant (block rule: 'sssd'). In each block, the tone duration was 200 ms, the inter-tone interval was 400 ms, and each sequence lasted 2000 ms, with a 1700 ms silent interval between sequences (Fig. S5). After this learning phase, each block concluded with a testing phase of 180 sequences. In each test phase, 135 sequences (75%) were congruent with the block rule (global standard), whereas 45 sequences (25%) violated the block rule (global deviant). At a minimum, at least two global standards were included between each global deviant, and the order of sequences in each testing phase was otherwise pseudorandomized. Each block was approximately 13 minutes in duration.

Because the fourth tone of each sequence can be compared to either other tones within the same sequence (local) or tones from the sequence introduced by the block rule (global), two levels of deviation are possible in this paradigm. For instance, given the block rule 'sssd', test phase sequence 'sssd' is a global standard but also a local deviant (i.e., the fourth tone is incongruent with the first three tones in its sequence—a first-order rule violation—but congruent with the global block rule sequence). Conversely, given the same block rule 'sssd', the test phase sequence 'sssS' (where the capital letter denotes a global rule violation) is a local standard but also a global deviant. For the block rule 'ssss', however, the test phase sequence 'sssD' is both a local and a global deviant. Given the hierarchical nature of the local-global paradigm, it is possible that first and second-order rule violations produce different sizes of cortical perturbations.

For additional details and protocols of this experiment, please see prior publications (*35*, *36*).

Data retention

Prior to preprocessing, MEG datasets were rejected from N = 4 participants in the fetal group and N = 6 participants in the neonatal group whose recordings were interrupted early. Of the remaining N = 56 participants in the fetal group, longitudinal recordings from N = 22 participants (N = 7 x two sessions, N = 3 x three sessions, and N = 12 x four sessions) were obtained. This yielded a total of 105 fetal datasets. Of these, fetal cortical signals were detected based on amplitude in 81 datasets which were retained (N = 24 x one session, N = 5 x two sessions, 9 x three sessions, N = 5 x four sessions) across 43 unique fetal subjects. Fetal cortical signals were identified based on a principal component approach and quality checked for consistency in location with fetal head position and overlap with remaining heart or muscle artifacts [see supplementary material of (*35*) for a detailed description of the process]. In the main analyses (i.e., all LMMs that included HRV as a predictor), six recordings missing usable MCG data were

excluded, resulting in 75 datasets from 41 subjects. Note that recordings without HRV were still retained for correlations (e.g., Fig. 1 and Fig. 4), and some previously excluded recordings were also utilized in the entropy decomposition (Table S1).

All recordings from newborns were cross-sectional. N = 6 newborns did not complete the full experiment, and thus data from N = 27 newborns entered preprocessing. After quality control, data from N = 20 newborns were retained.

For additional details of data preprocessing, please see prior publications (*35*, *36*).

Heart rate variability (HRV)

As a proxy for arousal level, HRV was measured in all fetal and neonatal data. R peaks were detected in the fetal/neonatal MCG signal prior to its removal from MEG data. The R peaks were then used to compute the normal-to-normal R-R intervals (*65*), the standard deviation of which (SDNN) was taken as our measure of HRV. SDNN was $\log_{10}$ transformed prior to statistical analysis to better approximate a Gaussian distribution.

MEG data analysis

Preprocessing of MEG data was conducted using MATLAB R2016b (The MathWorks, Natick, MA, USA). Fetal signals were bandpass filtered at 1-10 Hz and neonatal signals were bandpass filtered at 1-15 Hz prior to analysis, which is a typical filtering range for fetal and neonatal event related responses (*66*). For each fetal recording, a cluster of 10 channels with the highest signal amplitude after artifact removal were root mean square normalized and chosen for further analysis. Similarly, for each neonatal recording, five channels containing cortical signals were identified using principal component analysis and chosen for further analysis (*67*). Signals were segmented from -200 ms to +3000 ms referenced to the onset of the first tone (Fig. S5). To adjust for the excess number of standard trials in each block, only standard trials immediately preceding deviant trials were analyzed. Note that we did not examine shorter subsegments of trial-averaged signals (e.g., after the onset of the fourth tone) due to the lowpass filtering which limits the usefulness of shorter data segments (e.g., in fetal data lowpass filtered at 10 Hz, a 1000 ms subsegment would contain at most 10 oscillatory cycles).

Cortical entropy

Data analysis from this point forward was conducted using MATLAB R2021b/2022a. Entropy is an information-theoretic quantity which measures the degree of uncertainty (or unpredictability) in data generated by a given probability distribution. When applied to time series data, it can be interpreted as quantifying the degree of diversity in a signal: the higher a signal's entropy, the more it will explore different trajectories. It is also, in a sense, a measure of information, as highly entropic signals may have a greater informational content (Cover and Thomas, 2006). To estimate cortical entropy, we used several approaches applied to signals that had already been averaged

across trials and channels from each recording. First, we utilized the LZC (*68*) and CTW (*69*) compression algorithms, which determine the number of unique substrings in the signal, a quantity which relates to the signal's ground truth entropy (more technically, to its *entropy rate*) (*70*). Both approaches require the signal to be transformed into discrete symbols. For both LZC and CTW, we satisfied this requirement in a binary fashion by thresholding each signal using its median value.

Besides compression-based methods, we also utilized entropy estimates based on state-space reconstruction (*71*). These include the modified sample entropy (mSampEn) ; (*72*) and permutation entropy (PermEn) (*73*). The mSampEn reflects the tendency of motifs to reoccur within a signal (*74*). We also examined a variant of mSampEn, the modified multiscale sample entropy, or mMSE, which computes mSampEn at different timescales (*75*); specifically, we averaged mMSE across 20 timescales. Both mSampEn and mMSE were calculated using z-scored signals. The PermEn reflects the occurrence of unique permutations based on ordinal rankings of data (*73*). These ordinal rankings are created by choosing a lag or timescale to separate samples. We computed PermEn using two different lags (*38*, *76*) appropriate for our data: τ = 32 ms (PermEn32, sensitive to 4 - 10 Hz activity) and τ = 64 ms (PermEn64, sensitive to 2 - 5 Hz activity). All entropy measures were computed after averaging MEG channels of interest (see "Data retention" above).

Cortical dynamics

According to the entropic brain hypothesis, entropy levels exceeding a critical point may indicate diminishing, rather than increasing, levels of consciousness (*50*), e.g., if entropy represents cortical noise. Testing this hypothesis requires one to infer the dynamics of the signal. To investigate whether the dynamics of each cortical signals were stochastic (i.e., containing intrinsic randomness), or deterministic (i.e., predetermined by initial conditions, encompassing both periodic and chaotic behavior), we adapted a decision tree algorithm by Toker et al. (*45*). The algorithm infers whether signal dynamics are stochastic using two rounds of surrogate data testing with 1000 surrogates. For the first round, 1000 surrogates were generated using the iterative amplitude adjusted Fourier Transform method that exactly preserves the power spectrum (IAAFT-2). Additionally, to rule out the possibility of nonlinear stochasticity, a second round of surrogate data testing was performed using 1000 cyclic phase permutation surrogates. Because de-noising is crucial to the algorithm's success (*45*), we lowpass filtered signals from newborns again at a lower frequency (10 Hz, finite impulse response, filter order = 610) before classifying their dynamics. Having identified all signals as either stochastic or deterministic, LMMs were then used to predict signal dynamics (see "Statistical analysis" below).

Statistical analysis

To evaluate the effects of maturation and arousal on signal complexity, we used LMMs (with MATLAB's fitlme function) which accounted for longitudinal data. LMMs had the formula

COMPLEXITY ~ AGE + HRV + STIMULUS + RULE + STIMULUS*RULE + (1|PARTICIPANT) (1)

where COMPLEXITY is a value measuring signal entropy, AGE is the gestational age in weeks (fetal data) or postnatal age in days (neonatal data), HRV is the heart rate variability [measured as $\log_{10}$(SDNN)], STIMULUS is the stimulus type which varied depending on the fourth tone of the sequence (categorical variable: 'ssss' or 'sssd'), RULE is the global rule established in the exposure phase which varied depending on the block (takes the same values as STIMULUS), STIMULUS*RULE is the interaction of stimulus type and block rule that determines whether stimuli are global standards or global deviants, and the final term (1|PARTICIPANT) denotes random intercepts for each participant.

Next, to evaluate the effect of surrogacy on signal complexity measures (see "Surrogate data testing" below), we used LMMs with the formula

COMPLEXITY ~ SURROGACY + STIMULUS + RULE + STIMULUS*RULE + (1|PARTICIPANT) (2)

where SURROGACY is a binary variable indicating whether signals are surrogates.

Additionally, to evaluate the effects of maturation and arousal on signal dynamics, we used LMMs with the formula

DYNAMICS ~ AGE + HRV + STIMULUS + RULE + STIMULUS*RULE + (1|PARTICIPANT) (3)

where DYNAMICS is a categorical variable indicating the outcome of the decision tree for categorizing signal dynamics.

Finally, to evaluate ERSPs, we modeled spectral power from each element of the TFR using LMMs with the formula

POWER ~ AGE + HRV + STIMULUS + RULE + STIMULUS*RULE + (1|PARTICIPANT) (4)

where POWER is the $\log_{10}$(power) of the TFR element. In doing so, we faced a multiple comparisons problem as models were fit for thousands of elements in each interpolated TFR. We addressed this problem using permutation cluster statistics (*77*). For each of 2000 permutations, we randomly shuffled each predictor variable (AGE, HRV, STIMULUS, and RULE) in the LMM. For each predictor, positive and negative t-statistics were thresholded separately based on whether they corresponded to $p < 0.005$. We then identified clusters of t-statistics exceeding the threshold using the regionprops() function in MATLAB and measured the `intensity' of each cluster as the absolute value of the sum of the t-values of all regions within it.

For each permutation, the size of the largest cluster was saved, thus generating a permutation distribution of cluster sizes. We then applied the same procedure to the non-permuted data and derived an empirical p-value for each cluster by comparing the actual cluster size to the permutation distribution of cluster sizes.

More broadly, we faced another multiple comparisons problem stemming from multiple hypotheses tested across our analyses. To address this, we controlled the false discovery rate (FDR) using the Benjamini-Hochberg procedure to correct p-values (*42*).

Entropy decomposition

We used an entropy decomposition (*44*) to investigate the extent to which amplitude versus non-amplitude (i.e., phase and its interaction with amplitude) properties of the MEG signal contributed to changes in each entropy measure. The decomposition requires two sets of paired data to compute differences in entropy. In fetuses, we compared entropy between early versus late fetuses in subjects with longitudinal data both before and after 35 weeks. In newborns, which did not give longitudinal data, we split participants according to their median age and computed entropy differences based on all possible pairings of “young” and “old” newborns. In each group, we selected data from the condition that yielded the largest correlations between maturation and entropy (sssD in fetuses and sssS in newborns). For each signal, we generated 250 surrogates (*78*) by shuffling phases separately within younger versus and subjects in one procedure and then between younger and older subjects pooled together in another procedure. By applying the inverse Fourier transform to obtain surrogate signals from these shuffling procedures, the decomposition algorithm allows for the effects of amplitude, phase, and their interaction to be systematically disentangled, e.g., when phases are pooled between age groups, the difference that remains is due to amplitude. For full details of the algorithm, please refer to Mediano et al. (*44*).

As stated previously, newborn participants did not return to the laboratory for multiple visits, and thus natural pairings between neonatal recordings did not exist. As a workaround, for each of the older newborns, we computed the average difference between its entropy and that of the younger newborns; this procedure was then repeated with each of the younger newborns compared to older newborns. In other words, for the ith newborn in the younger subgroup, we

computed an entropy difference ΔH between its signal and the signal of all older newborns according to

$$\Delta H_i = \frac{1}{N}\sum_{j=1}^{N} H_i - H_j \quad (5)$$

where j indexes each of the older newborns. Similarly, for the jth newborn in the older subgroup, we computed ΔH between its signal and the signal of all younger newborns according to

$$\Delta H_j = \frac{1}{N}\sum_{i=1}^{N} H_i - H_j \quad (6)$$

and so we obtained one average difference for each participant, allowing us to ask which component of the entropy change was larger for each participant; note that the sum of ΔH_i across all N newborns in the younger subgroup equals the sum of ΔH_j across all N newborns in the older subgroup. To avoid artificially inflating our statistical power, we tested entropy differences separately for each subgroup, rather than pooling ΔH across the two subgroups. We then arbitrarily chose to report entropy difference referenced to the younger subgroup, while also confirming that the same finding persisted after referencing entropy differences to the older subgroup (see Fig. S2).

After decomposing entropy changes into amplitude, phase, and amplitude x phase interaction components for fetal and neonatal data, we summed the differences in each entropy measure attributable to phase and phase x amplitude interactions to create a single "non-amplitude" quantity which we compared to the difference in entropy attributable to amplitude using paired samples t-tests.

Surrogate data testing

To assess whether the entropy of cortical signals differed from that of noise with similar spectral properties (i.e., surrogate data), we utilized surrogate data testing (*78*, *79*). Surrogate signals were generated from each cortical signal using the iterative amplitude adjusted Fourier transform that exactly preserves the amplitude distribution (IAAFT-1) algorithm (*80*), resulting in signals with maximal entropy given a fixed variance (*70*). Note that we followed best practices by generating the surrogate signal after truncation of the original signal, so that start and end points had approximately the same value and same first derivative (*79*). The entropy of cortical signals was calculated separately with truncation only for the purpose of comparing with surrogates (i.e., elsewhere, we used the entropy computed from the full signal without truncation). For each cortical signal, entropy measures were also computed for each of 100 surrogate signals; the median entropy was then computed across all surrogates. To evaluate whether a given measure

differed between cortical and surrogate signals, we used LMMs (see “Statistical analysis” above) and evaluated the surrogacy term in each model.

Correlations between MEG measures

To investigate possible relationships amongst MEG measures, we examined correlations between signal entropy measures both with each other and with spectral power. For neonatal data, correlations were computed using Pearson correlation coefficients. Because fetal data show statistical dependencies between longitudinal recordings (see Table S3), we z-scored MEG measures from fetal data and used the normalized beta coefficients from random intercept regression models. Because standardized betas in LMMs depend on the variance of the random effect and are thus generally asymmetrical (i.e., $\beta_{i,j} \neq \beta_{j,i}$), we used the mean of $\beta_{i,j}$ and $\beta_{j,i}$ to represent the correlation between entropy measure i and j (Fig. S1). This was done using LMMs with the formula

$$\text{MEASURE1} \sim \text{MEASURE2} + (1|\text{PARTICIPANT}) \quad (7)$$

and

$$\text{MEASURE2} \sim \text{MEASURE1} + (1|\text{PARTICIPANT}) \quad (8)$$

and subsequently averaging the beta coefficient of MEASURE2 in Eq. 8 with that of MEASURE 1 in Eq. 9 to report the correlation strength, where MEASURE1 and MEASURE2 are the pair of MEG measures whose correlations is being determined. Note that because measures have unit variance after z-scoring, beta coefficients were bounded between -1 and 1.

Because our concern was mostly with correlation direction and size rather than statistical significance, we did not derive p-values for correlations. Besides investigating correlations across recordings, we also examined temporal correlations of CTW with spectral power after averaging the ERF across all datasets within each of four stimulus/rule conditions. A notable property of CTW is its superior temporal resolution over LZC due to its faster convergence, which can be used to evaluate sub-second changes in entropy (*81*). For this reason, we used time-resolved CTW with 164 ms (i.e., 100 sample) sliding windows with 90% overlap to evaluate correlations between entropy and spectral power on the grand-averaged ERFs. Spectral power was computed for grand-averaged ERFs as described above for ERSPs, except for correlations across datasets, in which case we used four wavelets per octave (rather than eight wavelets per octave) to limit the number of correlations.

Post hoc correlations between maturation and entropy

After running LMMs to predict entropy from maturation and other variables, we examined the correlation between maturation without the influence of covariates. Outlier values of each entropy measure more than 6 median absolute deviations from the median value across both stimuli and block rules were discarded before running correlations. As described above, in fetuses with longitudinal data, we z-scored both gestational ages and entropy measures and used a random intercept model with the formula

$$\text{ENTROPY} \sim \text{AGE} + (1|\text{PARTICIPANT}) \quad (9)$$

to derive a correlation using the beta coefficient of the AGE term (again, $-1 \leq \beta \leq 1$). For newborns, we derived correlations using Pearson coefficients.

Event related spectral perturbation (ERSPs)

To compute ERSPs that map cortical responses to tones in frequency and time, we used Morlet wavelets with 8 wavelets per octave, yielding a total of 27 wavelets logarithmically spaced from 1 to 10 Hz (fetal data) and 32 wavelets logarithmically spaced from 1 to 15 Hz (neonatal data). For all frequencies, sliding windows used for the wavelet transform overlapped by 90% and decayed exponential in length as a function of $\log_2$(frequency). Time frequency representations (TFRs) obtained from Morlet wavelets were linearly interpolated to increase TFR size. For fetal data, this resulted in a conversion from 23 x 27 bins to 177 x 209 bins (-200 - 3000 ms, time referenced to the first tone) x frequency (1.00 - 9.51 Hz). For neonatal data, this resulted in a conversion from 23 x 32 bins to 177 x 249 bins (-200 - 3000 ms, time referenced to the first tone) x frequency (1.00 - 14.7 Hz).

Acknowledgements

We are grateful to all volunteers and families who participated in our research. We would also like to thank Daniel Toker for his input on methodological aspects of our study, Alessandra Alessandra DallaVecchia for her input on “sensory PCI”, and Simon Ruch for assisting with a code review. Finally, we thank the fMEG team for their contributions, including Franziska Schleger (original study design), Magdalene Weiss (data collection), and Katrin Sippel (data processing).

We gratefully acknowledge the following funders: 1) the FET Open Luminous project (H2020 FETOPEN-2014-2015-RIA under agreement No. 686764) as part of the European Union’s Horizon 2020 research and 2014 – 2018 training program, 2) the German Federal Ministry of Education and Research (BMBF) to the German Center for Diabetes Research (DZD01GI0925), 3) the Deutsche Forschungsgemeinschaft (DFG, German Research Foundation; 493345456), 4) the Wellcome Trust (grant no. 210920/Z/18/Z), and 5) the Open Access Publishing Fund of the University of Tübingen.

Financial disclosures

The authors report no financial conflicts of interest.

References

1. S. Sarasso, A. G. Casali, S. Casarotto, M. Rosanova, C. Sinigaglia, M. Massimini, Consciousness and complexity: a consilience of evidence. *Neuroscience of Consciousness* (2021).

2. A. G. Casali, O. Gosseries, M. Rosanova, M. Boly, S. Sarasso, K. R. Casali, S. Casarotto, M.-A. Bruno, S. Laureys, G. Tononi, A theoretically based index of consciousness independent of sensory processing and behavior. *Science translational medicine*. **5**, 198ra105-198ra105 (2013).

3. M. M. Schartner, A. Pigorini, S. A. Gibbs, G. Arnulfo, S. Sarasso, L. Barnett, L. Nobili, M. Massimini, A. K. Seth, A. B. Barrett, Global and local complexity of intracranial EEG decreases during NREM sleep. *Neuroscience of consciousness*. **2017**, niw022 (2017).

4. S. Sarasso, M. Boly, M. Napolitani, O. Gosseries, V. Charland-Verville, S. Casarotto, M. Rosanova, A. G. Casali, J.-F. Brichant, P. Boveroux, Consciousness and complexity during unresponsiveness induced by propofol, xenon, and ketamine. *Current Biology*. **25**, 3099–3105 (2015).

5. M. Schartner, A. Seth, Q. Noirhomme, M. Boly, M.-A. Bruno, S. Laureys, A. Barrett, Complexity of multi-dimensional spontaneous EEG decreases during propofol induced general anaesthesia. *PloS one*. **10**, e0133532 (2015).

6. S. Casarotto, A. Comanducci, M. Rosanova, S. Sarasso, M. Fecchio, M. Napolitani, A. Pigorini, A. G. Casali, P. D. Trimarchi, M. Boly, Stratification of unresponsive patients by an independently validated index of brain complexity. *Annals of neurology*. **80**, 718–729 (2016).

7. M. M. Schartner, R. L. Carhart-Harris, A. B. Barrett, A. K. Seth, S. D. Muthukumaraswamy, Increased spontaneous MEG signal diversity for psychoactive doses of ketamine, LSD and psilocybin. *Scientific Reports*. **7**, 46421 (2017).

8. N. Farnes, B. E. Juel, A. S. Nilsen, L. G. Romundstad, J. F. Storm, Increased signal diversity/complexity of spontaneous EEG, but not evoked EEG responses, in ketamine-induced psychedelic state in humans. *Plos one*. **15**, e0242056 (2020).

9. B. Baird, G. Tononi, S. LaBerge, Lucid dreaming occurs in activated rapid eye movement sleep, not a mixture of sleep and wakefulness. *Sleep* (2022).

10. J. Frohlich, J. N. Chiang, P. A. Mediano, M. Nespeca, V. Saravanapandian, D. Toker, J. Dell'Italia, J. F. Hipp, S. S. Jeste, C. J. Chu, L. M. Bird, M. M. Monti, Neural Complexity is a Common Denominator of Human Consciousness Across Diverse Regimes of Cortical Dynamics (2022), , doi:https://dx.doi.org/10.2139/ssrn.4056850.

11. D. Abásolo, R. Hornero, P. Espino, D. Alvarez, J. Poza, Entropy analysis of the EEG background activity in Alzheimer's disease patients. *Physiological measurement*. **27**, 241 (2006).

12. D. Abásolo, R. Hornero, P. Espino, J. Poza, C. I. Sánchez, R. de la Rosa, Analysis of regularity in the EEG background activity of Alzheimer's disease patients with Approximate Entropy. *Clinical neurophysiology*. **116**, 1826–1834 (2005).

13. A. C. Yang, C.-C. Huang, H.-L. Yeh, M.-E. Liu, C.-J. Hong, P.-C. Tu, J.-F. Chen, N. E. Huang, C.-K. Peng, C.-P. Lin, Complexity of spontaneous BOLD activity in default mode network is correlated with cognitive function in normal male elderly: a multiscale entropy analysis. *Neurobiology of aging*. **34**, 428–438 (2013).

14. W. J. Bosl, H. Tager-Flusberg, C. A. Nelson, EEG analytics for early detection of autism spectrum disorder: a data-driven approach. *Scientific reports*. **8**, 1–20 (2018).

15. W. Bosl, A. Tierney, H. Tager-Flusberg, C. Nelson, EEG complexity as a biomarker for autism spectrum disorder risk. *BMC medicine*. **9**, 1–16 (2011).

16. M. Lavanga, J. De Ridder, K. Kotulska, R. Moavero, P. Curatolo, B. Weschke, K. Riney, M. Feucht, P. Krsek, R. Nabbout, Results of quantitative EEG analysis are associated with autism spectrum disorder and development abnormalities in infants with tuberous sclerosis complex. *Biomedical Signal Processing and Control*. **68**, 102658 (2021).

17. J. Monge, C. Gómez, J. Poza, A. Fernández, J. Quintero, R. Hornero, MEG analysis of neural dynamics in attention-deficit/hyperactivity disorder with fuzzy entropy. *Medical engineering & physics*. **37**, 416–423 (2015).

18. M. O. Sokunbi, W. Fung, V. Sawlani, S. Choppin, D. E. Linden, J. Thome, Resting state fMRI entropy probes complexity of brain activity in adults with ADHD. *Psychiatry Research: Neuroimaging*. **214**, 341–348 (2013).

19. D. Bai, W. Yao, S. Wang, J. Wang, Multiscale Weighted Permutation Entropy Analysis of Schizophrenia Magnetoencephalograms. *Entropy*. **24**, 314 (2022).

20. T. Takahashi, R. Y. Cho, T. Mizuno, M. Kikuchi, T. Murata, K. Takahashi, Y. Wada, Antipsychotics reverse abnormal EEG complexity in drug-naive schizophrenia: a multiscale entropy analysis. *Neuroimage*. **51**, 173–182 (2010).

21. P. C. Ivanov, L. A. N. Amaral, A. L. Goldberger, S. Havlin, M. G. Rosenblum, Z. R. Struzik, H. E. Stanley, Multifractality in human heartbeat dynamics. *Nature*. **399**, 461–465 (1999).

22. C.-S. Poon, C. K. Merrill, Decrease of cardiac chaos in congestive heart failure. *Nature*. **389**, 492–495 (1997).

23. H.-B. Xie, J.-Y. Guo, Y.-P. Zheng, Fuzzy approximate entropy analysis of chaotic and natural complex systems: detecting muscle fatigue using electromyography signals. *Annals of biomedical engineering*. **38**, 1483–1496 (2010).

24. J. Frohlich, The fugue of life: why complexity matters in neuroscience. *Aeon* (2016), (available at https://aeon.co/ideas/the-fugue-of-life-why-complexity-matters-in-neuroscience).

25. S. Janjarasjitt, M. Scher, K. Loparo, Nonlinear dynamical analysis of the neonatal EEG time series: the relationship between sleep state and complexity. *Clinical neurophysiology*. **119**, 1812–1823 (2008).

26. M. S. Scher, H. Waisanen, K. Loparo, M. W. Johnson, Prediction of neonatal state and maturational change using dimensional analysis. *Journal of clinical neurophysiology*. **22**, 159–165 (2005).

27. F. Kaffashi, M. Scher, S. Ludington-Hoe, K. Loparo, An analysis of the kangaroo care intervention using neonatal EEG complexity: a preliminary study. *Clinical neurophysiology*. **124**, 238–246 (2013).

28. J. R. Isler, R. I. Stark, P. G. Grieve, M. G. Welch, M. M. Myers, Integrated information in the EEG of preterm infants increases with family nurture intervention, age, and conscious state. *PloS One*. **13**, e0206237 (2018).

29. G. Tononi, M. Boly, M. Massimini, C. Koch, Integrated information theory: from consciousness to its physical substrate. *Nature Reviews Neuroscience*. **17**, 450–461 (2016).

30. J. Frohlich, A. Irimia, S. S. Jeste, Trajectory of frequency stability in typical development. *Brain imaging and behavior*. **9**, 5–18 (2015).

31. S. Lippé, N. Kovacevic, R. McIntosh, Differential maturation of brain signal complexity in the human auditory and visual system. *Frontiers in human neuroscience*. **3**, 48 (2009).

32. A. R. McIntosh, N. Kovacevic, R. J. Itier, Increased brain signal variability accompanies lower behavioral variability in development. *PLoS computational biology*. **4**, e1000106 (2008).

33. B. Mišic, T. Mills, M. J. Taylor, A. R. McIntosh, Brain noise is task dependent and region specific. *Journal of Neurophysiology*. **104**, 2667–2676 (2010).

34. J. Moser, S. Bensaid, E. Kroupi, F. Schleger, F. Wendling, G. Ruffini, H. Preißl, Evaluating Complexity of Fetal MEG Signals: A Comparison of Different Metrics and Their Applicability. *Frontiers in systems neuroscience*. **13**, 23 (2019).

35. J. Moser, F. Schleger, M. Weiss, K. Sippel, L. Semeia, H. Preissl, Magnetoencephalographic signatures of conscious processing before birth. *Developmental cognitive neuroscience*. **49**, 100964 (2021).

36. J. Moser, F. Schleger, M. Weiss, K. Sippel, G. Dehaene-Lambertz, H. Preissl, Magnetoencephalographic signatures of hierarchical rule learning in newborns. *Developmental cognitive neuroscience*. **46**, 100871 (2020).

37. T. A. Bekinschtein, S. Dehaene, B. Rohaut, F. Tadel, L. Cohen, L. Naccache, Neural signature of the conscious processing of auditory regularities. *Proceedings of the National Academy of Sciences*. **106**, 1672–1677 (2009).

38. J.-R. King, J. D. Sitt, F. Faugeras, B. Rohaut, I. El Karoui, L. Cohen, L. Naccache, S. Dehaene, Information sharing in the brain indexes consciousness in noncommunicative patients. *Current Biology*. **23**, 1914–1919 (2013).

39. J. D. Sitt, J.-R. King, I. El Karoui, B. Rohaut, F. Faugeras, A. Gramfort, L. Cohen, M. Sigman, S. Dehaene, L. Naccache, Large scale screening of neural signatures of consciousness in patients in a vegetative or minimally conscious state. *Brain*. **137**, 2258–2270 (2014).

40. L. Semeia, K. Sippel, J. Moser, H. Preissl, Evaluation of parameters for fetal behavioural state classification. *Scientific reports*. **12**, 1–10 (2022).

41. J. Frohlich, T. Bayne, A. DallaVecchia, A. Kirkeby-Hinrup, P. A. Mediano, J. Moser, K. Talar, A. Gharabaghi, H. Preissl, Not with a “zap” but with a “beep”: measuring the origins of perinatal experience (2022).

42. Y. Benjamini, Y. Hochberg, Controlling the false discovery rate: a practical and powerful approach to multiple testing. *Journal of the Royal statistical society: series B (Methodological)*. **57**, 289–300 (1995).

43. P. J. Marshall, Y. Bar-Haim, N. A. Fox, Development of the EEG from 5 months to 4 years of age. *Clinical neurophysiology*. **113**, 1199–1208 (2002).

44. P. A. Mediano, F. E. Rosas, A. B. Barrett, D. Bor, Decomposing spectral and phasic differences in non-linear features between datasets. *arXiv preprint arXiv:2009.10015* (2020).

45. D. Toker, F. T. Sommer, M. D’Esposito, A simple method for detecting chaos in nature. *Communications biology*. **3**, 1–13 (2020).

46. A. Dallavecchia, F. Micheli, D. Toker, J. Frohlich, M. Monti, "Quantifying changes in complexity of the event related response to sensory stimuli in different states of arousal" in *SfN Global Connectome* (Virtual Conference, 2021).

47. M. Massimini, F. Ferrarelli, R. Huber, S. K. Esser, H. Singh, G. Tononi, Breakdown of cortical effective connectivity during sleep. *Science*. **309**, 2228–2232 (2005).

48. C. Bledowski, D. Prvulovic, R. Goebel, F. E. Zanella, D. E. Linden, Attentional systems in target and distractor processing: a combined ERP and fMRI study. *Neuroimage*. **22**, 530–540 (2004).

49. D. Sulcova, A. Salatino, A. Ivanoiu, A. Mouraux, Investigating the origin of TMS-evoked brain potentials using topographic analysis. *Brain Topography*, 1–16 (2022).

50. R. L. Carhart-Harris, The entropic brain-revisited. *Neuropharmacology*. **142**, 167–178 (2018).

51. R. L. Carhart-Harris, R. Leech, P. J. Hellyer, M. Shanahan, A. Feilding, E. Tagliazucchi, D. R. Chialvo, D. Nutt, The entropic brain: a theory of conscious states informed by neuroimaging research with psychedelic drugs. *Frontiers in human neuroscience*. **8**, 20 (2014).

52. J. Frohlich, L. M. Bird, J. Dell'Italia, M. A. Johnson, J. F. Hipp, M. M. Monti, High-voltage, diffuse delta rhythms coincide with wakeful consciousness and complexity in Angelman syndrome. *Neuroscience of consciousness*. **2020**, niaa005 (2020).

53. T. Rabinowicz, G. M. de Courten-Myers, J. M.-C. Petetot, G. Xi, E. de los Reyes, Human cortex development: estimates of neuronal numbers indicate major loss late during gestation. *Journal of neuropathology and experimental neurology*. **55**, 320–328 (1996).

54. S. Laureys, The neural correlate of (un) awareness: lessons from the vegetative state. *Trends in cognitive sciences*. **9**, 556–559 (2005).

55. F. Mormann, C. Koch, Neural correlates of consciousness. *Scholarpedia*. **2**, 1740 (2007).

56. M. Debnath, G. Venkatasubramanian, M. Berk, Fetal programming of schizophrenia: select mechanisms. *Neuroscience & Biobehavioral Reviews*. **49**, 90–104 (2015).

57. R. C. Knickmeyer, S. Baron-Cohen, Topical review: fetal testosterone and sex differences in typical social development and in autism. *Journal of child neurology*. **21**, 825–845 (2006).

58. A. S. Brown, Epidemiologic studies of exposure to prenatal infection and risk of schizophrenia and autism. *Developmental neurobiology*. **72**, 1272–1276 (2012).

59. M. S. Keshavan, S. Anderson, J. W. Pettergrew, Is schizophrenia due to excessive synaptic pruning in the prefrontal cortex? The Feinberg hypothesis revisited. *Journal of psychiatric research*. **28**, 239–265 (1994).

60. M. S. Thomas, R. Davis, A. Karmiloff-Smith, V. C. Knowland, T. Charman, The over-pruning hypothesis of autism. *Developmental Science*. **19**, 284–305 (2016).

61. C. M. Corsello, Early intervention in autism. *Infants & young children*. **18**, 74–85 (2005).

62. E. Boto, S. S. Meyer, V. Shah, O. Alem, S. Knappe, P. Kruger, T. M. Fromhold, M. Lim, P. M. Glover, P. G. Morris, A new generation of magnetoencephalography: Room temperature measurements using optically-pumped magnetometers. *NeuroImage*. **149**, 404–414 (2017).

63. R. T. Wakai, "Current Status and Future Prospects of Perinatal MEG" in *Magnetoencephalography* (Springer, 2014), pp. 641–644.

64. M. J. Brookes, J. Leggett, M. Rea, R. M. Hill, N. Holmes, E. Boto, R. Bowtell, Magnetoencephalography with optically pumped magnetometers (OPM-MEG): the next generation of functional neuroimaging. *Trends in Neurosciences* (2022).

65. H. Mat Husin, F. Schleger, I. Bauer, E. Fehlert, I. Kiefer-Schmidt, M. Weiss, K. O. Kagan, S. Brucker, J. Pauluschke-Fröhlich, H. Eswaran, Maternal weight, weight gain, and metabolism are associated with changes in fetal heart rate and variability. *Obesity*. **28**, 114–121 (2020).

66. F. Schleger, K. Landerl, J. Muenssinger, R. Draganova, M. Reinl, I. Kiefer-Schmidt, M. Weiss, A. Wacker-Gußmann, M. Huotilainen, H. Preissl, Magnetoencephalographic

signatures of numerosity discrimination in fetuses and neonates. *Developmental neuropsychology*. **39**, 316–329 (2014).

67. J. Moser, K. Sippel, F. Schleger, H. Preißl, "Automated Detection of Fetal Brain Signals with Principal Component Analysis" in (IEEE, 2019), pp. 6549–6552.

68. A. Lempel, J. Ziv, On the complexity of finite sequences. *IEEE Transactions on information theory*. **22**, 75–81 (1976).

69. F. M. Willems, Y. M. Shtarkov, T. J. Tjalkens, The context-tree weighting method: Basic properties. *IEEE transactions on information theory*. **41**, 653–664 (1995).

70. T. M. Cover, J. A. Thomas, *Elements of information theory* (John Wiley & Sons, 2012).

71. C. J. Stam, Nonlinear dynamical analysis of EEG and MEG: review of an emerging field. *Clinical neurophysiology*. **116**, 2266–2301 (2005).

72. H.-B. Xie, W.-X. He, H. Liu, Measuring time series regularity using nonlinear similarity-based sample entropy. *Physics Letters A*. **372**, 7140–7146 (2008).

73. C. Bandt, B. Pompe, Permutation entropy: a natural complexity measure for time series. *Physical review letters*. **88**, 174102 (2002).

74. J. S. Richman, J. R. Moorman, Physiological time-series analysis using approximate entropy and sample entropy. *American Journal of Physiology-Heart and Circulatory Physiology*. **278**, H2039–H2049 (2000).

75. M. Costa, A. L. Goldberger, C.-K. Peng, Multiscale entropy analysis of complex physiologic time series. *Physical review letters*. **89**, 068102 (2002).

76. P. Bourdillon, B. Hermann, M. Guénot, H. Bastuji, J. Isnard, J.-R. King, J. Sitt, L. Naccache, Brain-scale cortico-cortical functional connectivity in the delta-theta band is a robust signature of conscious states: an intracranial and scalp EEG study. *Scientific Reports*. **10**, 1–13 (2020).

77. E. Maris, R. Oostenveld, Nonparametric statistical testing of EEG-and MEG-data. *Journal of neuroscience methods*. **164**, 177–190 (2007).

78. J. Theiler, S. Eubank, A. Longtin, B. Galdrikian, J. D. Farmer, Testing for nonlinearity in time series: the method of surrogate data. *Physica D: Nonlinear Phenomena*. **58**, 77–94 (1992).

79. G. Lancaster, D. Iatsenko, A. Pidde, V. Ticcinelli, A. Stefanovska, Surrogate data for hypothesis testing of physical systems. *Physics Reports*. **748**, 1–60 (2018).

80. T. Schreiber, A. Schmitz, Improved surrogate data for nonlinearity tests. *Physical review letters*. **77**, 635 (1996).

81. Y. Gao, I. Kontoyiannis, E. Bienenstock, Estimating the entropy of binary time series: Methodology, some theory and a simulation study. *Entropy*. **10**, 71–99 (2008).

Figures

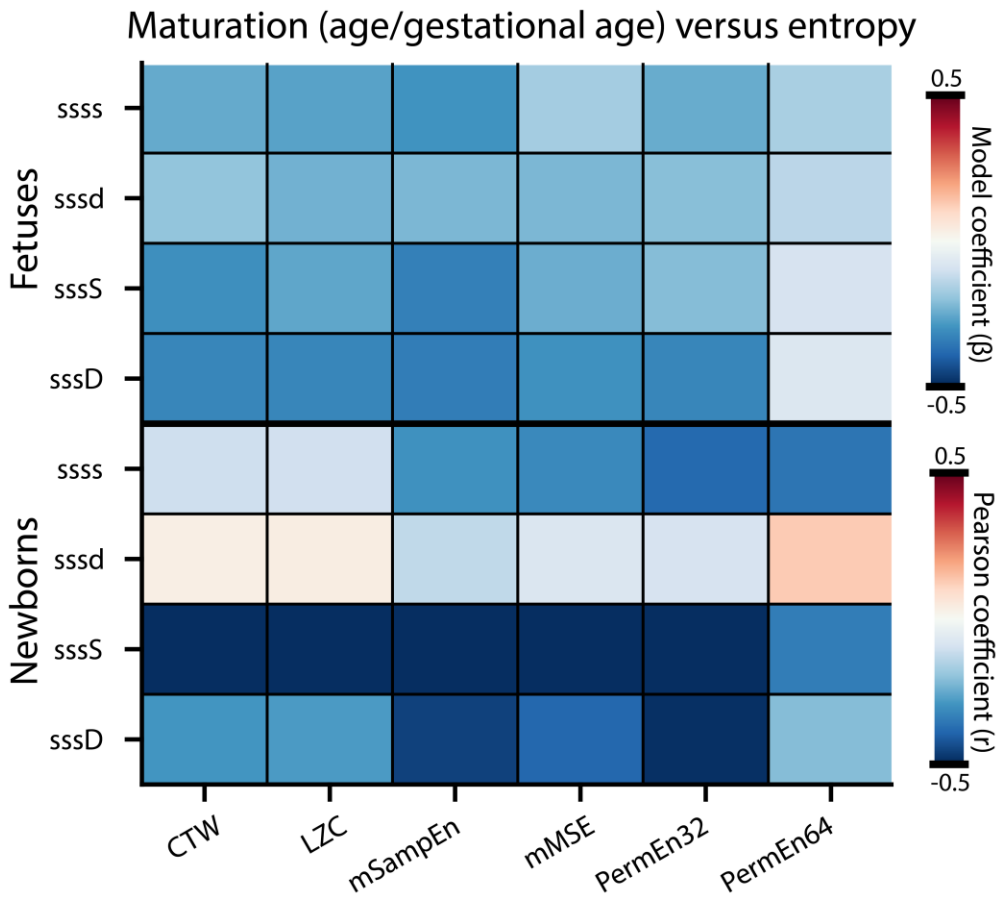

Figure 1 Post-hoc correlations between maturation and entropy in fetuses and newborns. Correlations were measured using model coefficients derived from z-scored data (fetuses) or from the Pearson correlation coefficient (newborns) after removing entropy outliers move than 6 median absolute deviations from the median of the distribution. All data were used that fell within 6 median absolute deviations from the median with entropy value (i.e., including recordings without usable MCG data). Maturation was defined as gestational age in fetuses (top four rows) and age in newborns (bottom four rows). We found that correlations between maturation and entropy are mostly negative. In fetuses, the strongest correlations were yielded by the sssD condition. Despite the fact that only one entropy measure (PermEn32) was significantly predicted by age in newborns, the strongest correlations between maturation and entropy were found in newborns (see Discussion for speculative explanations).

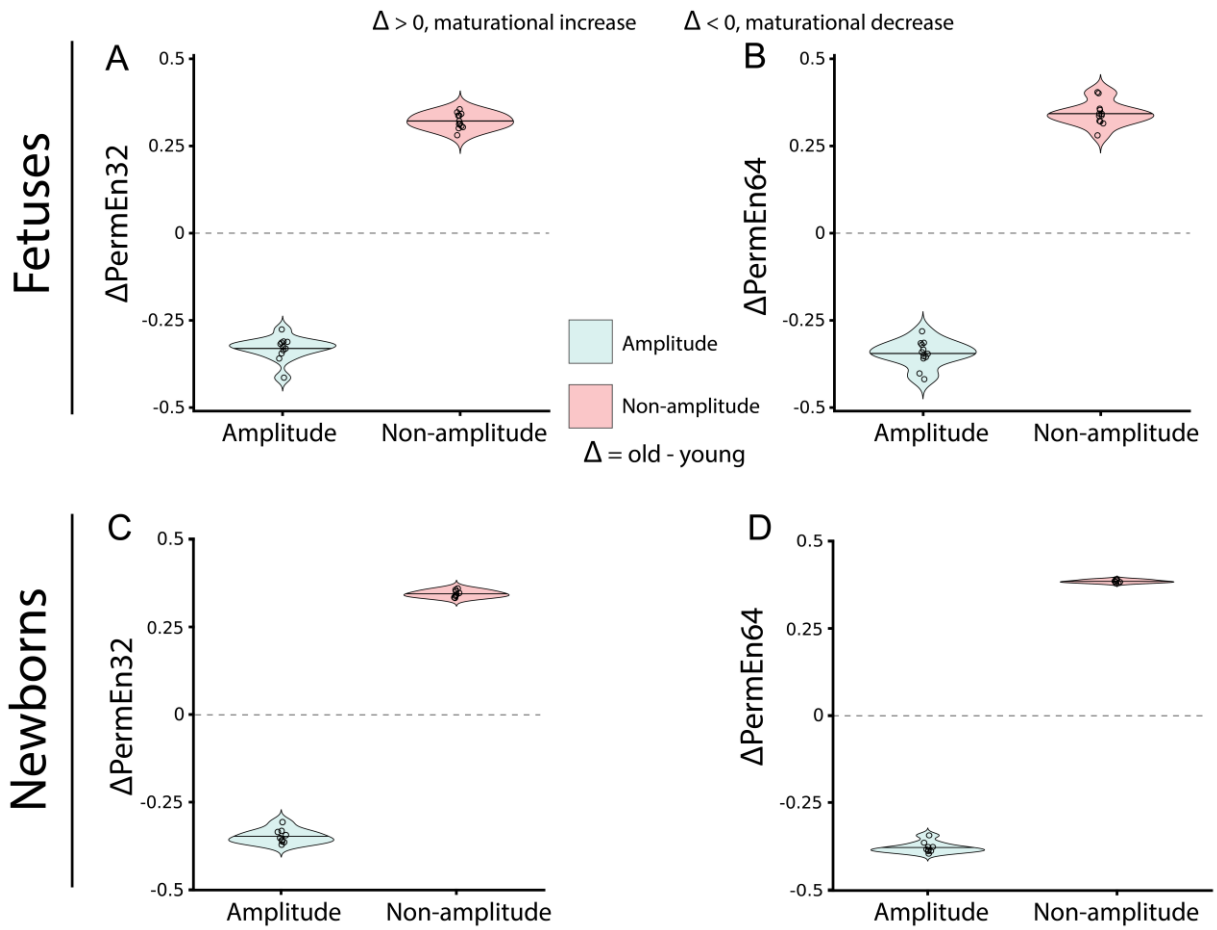

Figure 2 Changes in PermEn (old - young) attributable to amplitude versus non-amplitude (phase + phase x amplitude interaction) components of the MEG signal. (A,B) Data from 12 fetuses with MEG recordings at both early (< 35 weeks gestational age) and late (≥ 35 weeks gestational age) timepoints in the sssD condition. (C,D) Data from 9 newborns younger than 33 days were compared to data from 9 newborns older than 33 days of age in the sssS condition; the average difference in PermEn between each newborn in the younger group and all older newborns was then compared between amplitude and non-amplitude components. In both fetuses and newborns, PermEn32 and PermEn64 show a pattern by which amplitude and non-amplitude changes exert opposite influences on entropy, with the former being responsible for the overall decline in entropy with maturation that we detected in the main analysis using linear mixed models. The amplitude component of the PermEn changes is significantly greater than the non-amplitude component ($P_{FDR} < 10^{-10}$) in all cases.

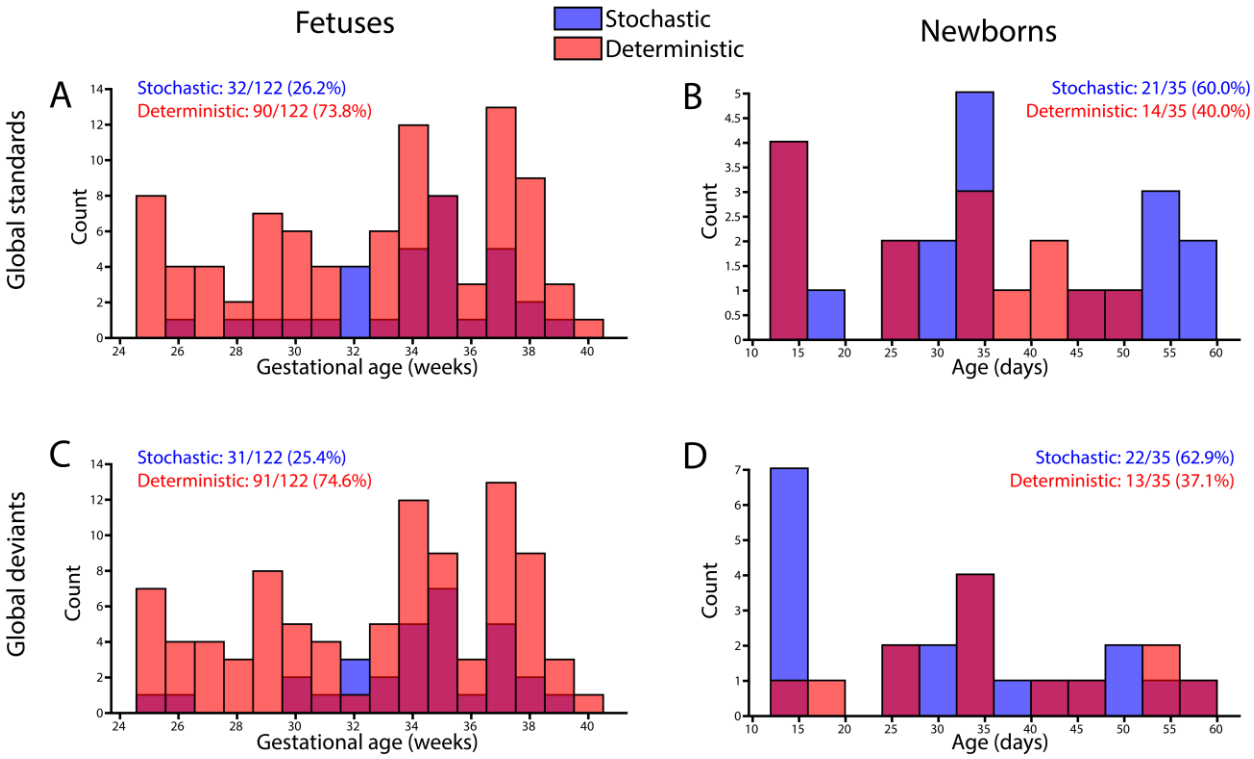

Figure 3 Histograms of signal dynamics categories (stochastic or deterministic) by gestational age (fetuses, left column) and age (newborns, right column). The first two rows show results from global standards (A, B) and the second row shows results from global deviants (C, D). Both fetuses and newborns displayed a mixture of stochastic and deterministic dynamics. In fetuses, the majority of recordings were deterministic, whereas in newborns, the majority of recordings were stochastic. Dynamics were not significantly predicted by maturation in either group, though the proportion of recordings with stochastic dynamics was significantly higher in newborns than in fetuses (chi-squared test, $\chi^2 = 30.8$, $p = 2.8 \times 10^{-8}$).

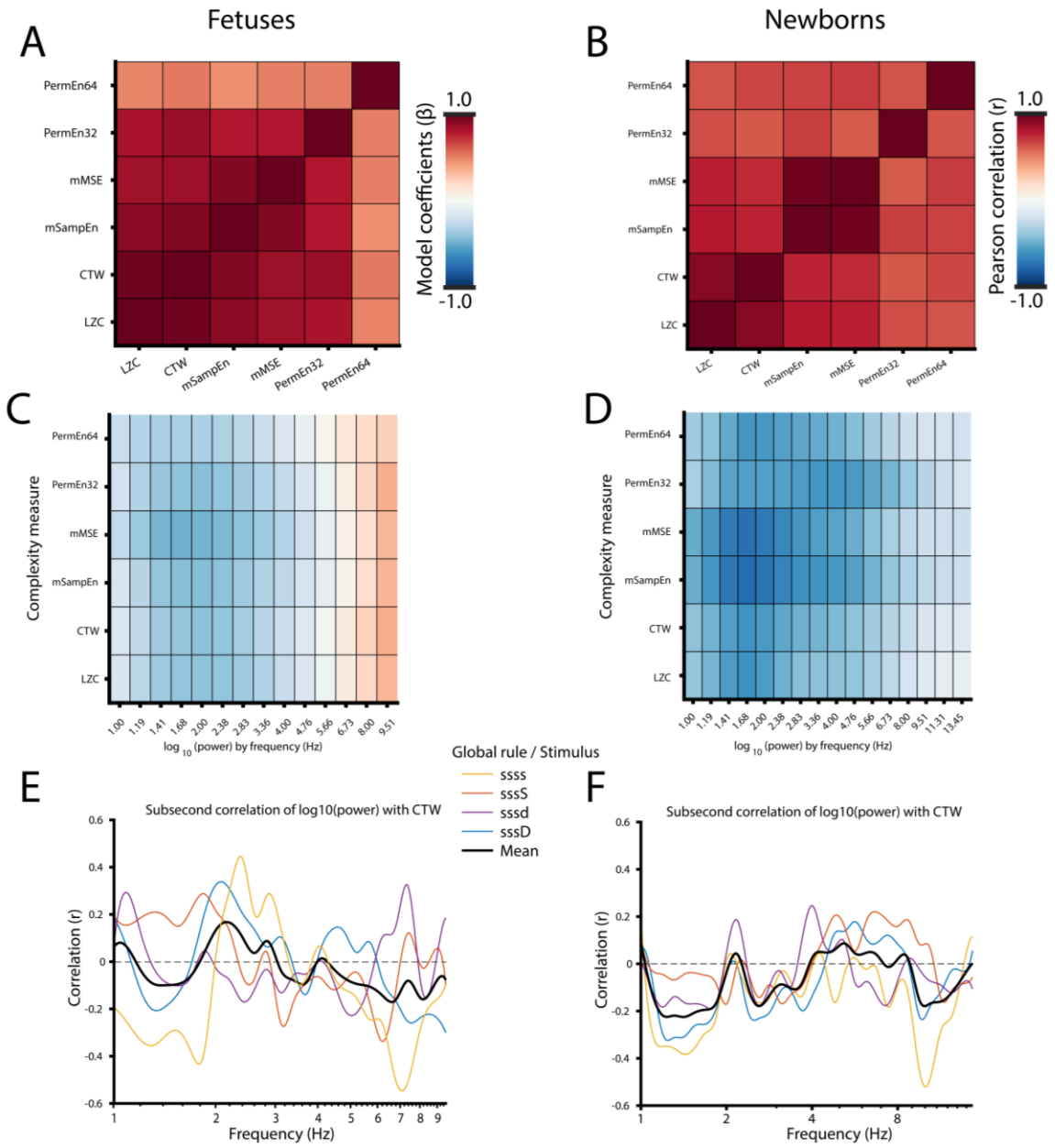

Figure 4 Correlations between MEG measures. Entropy measures were highly correlated with one another in both fetuses (A) and newborns (B). These same entropy measures show negative correlations with spectral power at most frequencies in fetuses (C) and all frequencies in newborns (D). Subsecond CTW did not correlate strongly with subsecond spectral power after averaging across conditions in fetuses (E) or newborns (F). Note than because some fetuses had longitudinal data, correlation coefficients in (E) were first averaged within subjects and then between subjects to make sure that fetuses with longitudinal data were not over-represented.

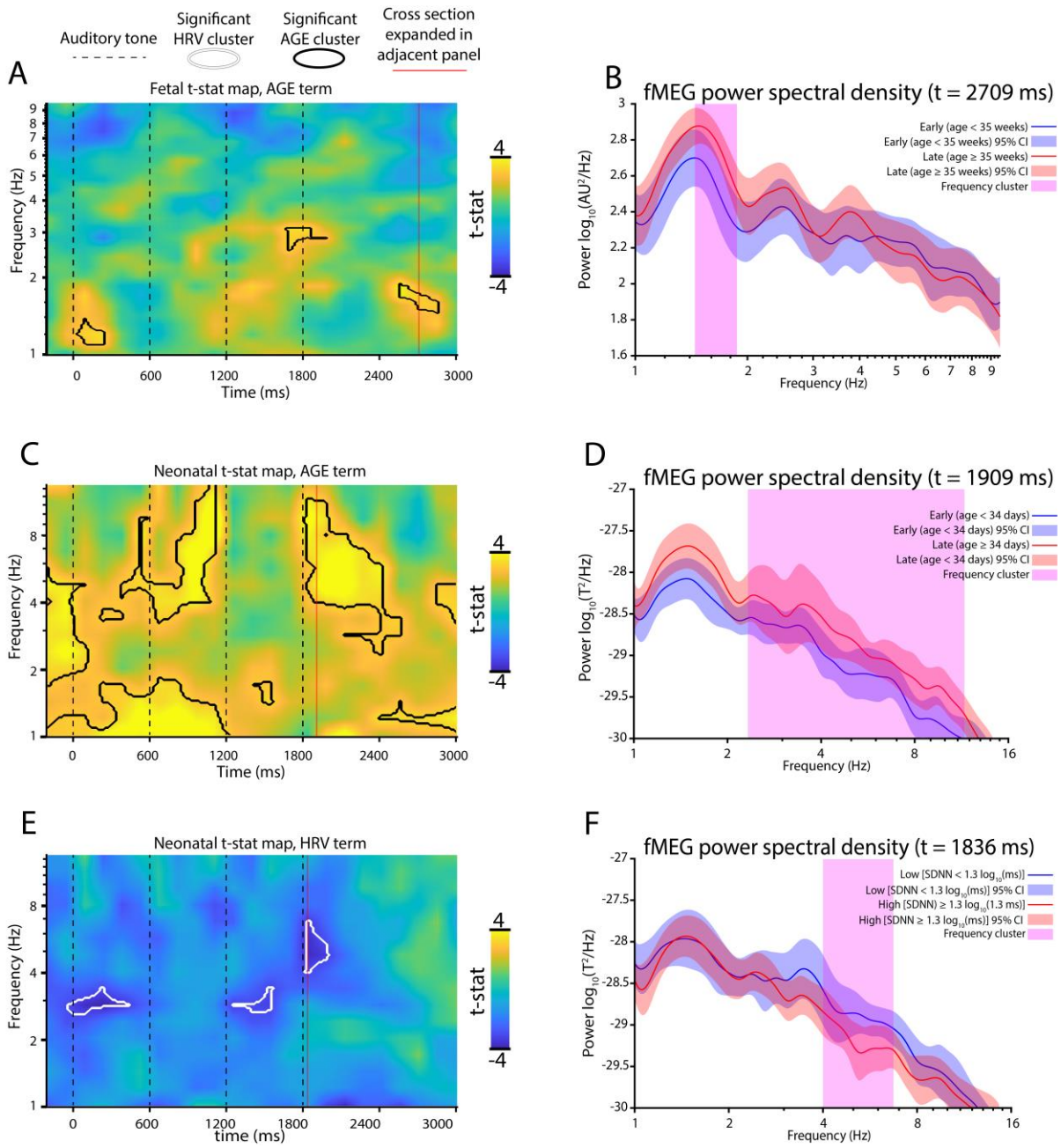

Figure 5 Significant clusters in fetal and neonatal time-frequency representations (TFRs). The left column displays time-frequency maps of t-statistics from linear mixed models (LMMs), with statistically significant clusters outlined in black or (AGE term) or white (HRV term). Red vertical lines indicate the widest cross sections of the largest cluster in each left-column panel, which correspond to power spectral densities displayed in the right column (pink highlights indicate the frequency extent of the cluster). In fetal data, we identified three significant clusters of greater power with gestational age (A, black contours, see Table 4 for cluster details). Based on Moser et al. (2021), we split fetal recordings for visualization purposes based on a gestational age of 35 weeks at which fetal cortical responses mature. Fetal recordings of at least this gestational age formed a group with greater low frequency power (delta band, between 1 and 2 Hz) at t = 2709

ms (B) than fetal recordings obtained below this gestational age. In neonatal recordings, we also found eight significant clusters corresponding to greater spectral power with age (C). We divided neonatal data based on a median split and found greater spectral power across a broad frequency range (D) in newborns with an age of at least 33 days versus younger newborns at a cross section of t = 1909 ms (just after the fourth tone). Additionally, we detected three significant clusters corresponding to greater spectral power with lower arousal in newborns (E). Using a median split for SDNN, we observed greater spectral power in the delta band (~3 Hz) in newborns with lower arousal [$\log_{10}$(ms) < 1.3] versus higher arousal at a cross section of t = 1836 ms (just after the fourth tone).

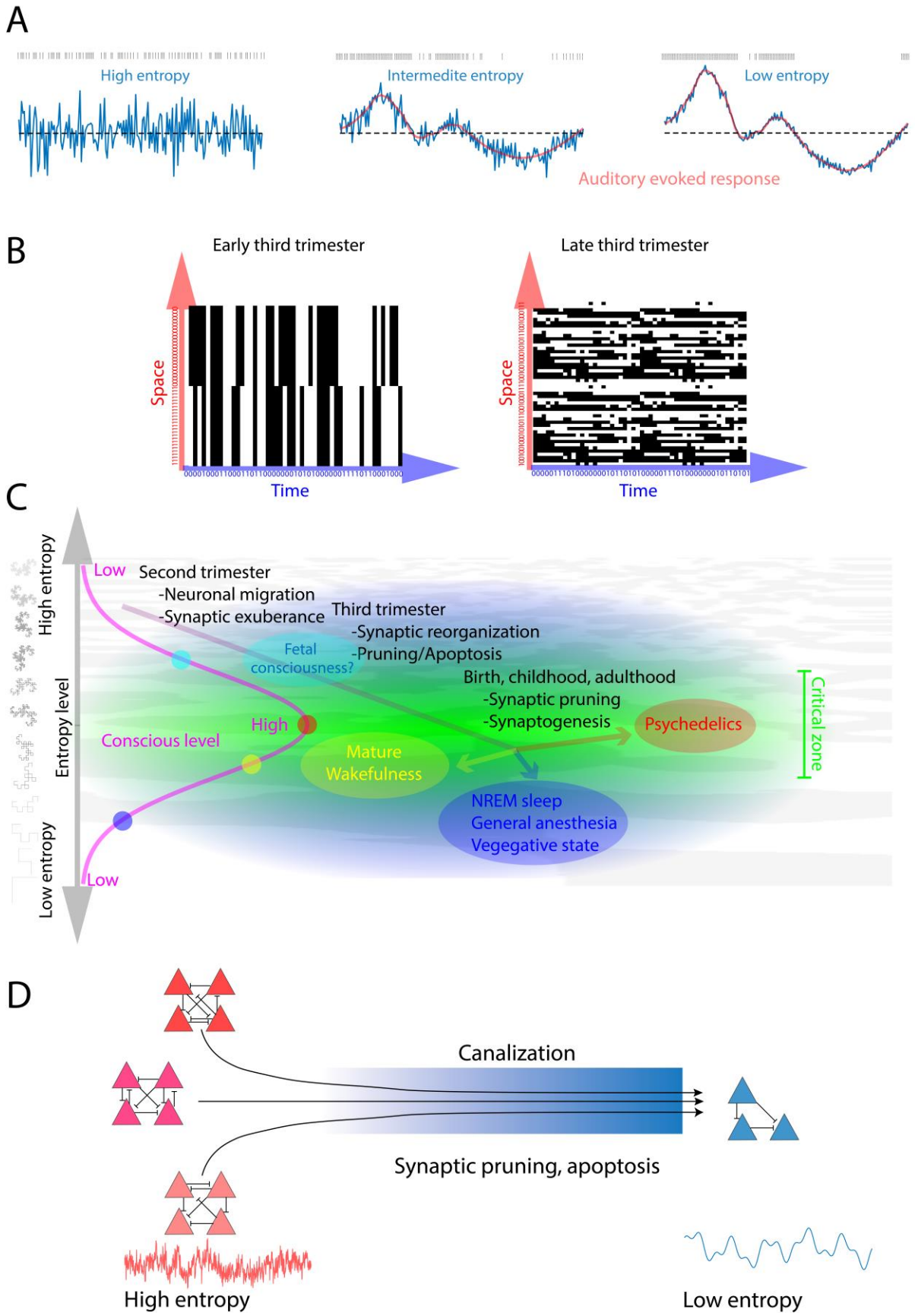
A
High entropy
Intermedite entropy
Low entropy
Auditory evoked response
B
Early third trimester
Late third trimester
Space
Time
Space
Time
C
High entropy
Entropy level
Low entropy
Low
Second trimester
-Neuronal migration
-Synaptic exuberance
Third trimester
-Synaptic reorganization
-Pruning/Apoptosis
Fetal consciousness?
Birth, childhood, adulthood
-Synaptic pruning
-Synaptogenesis
Psychedelics
Critical zone
High
Conscious level
Mature Wakefulness
NREM sleep
General anesthesia
Vegegative state
Low
D
Canalization
Synaptic pruning, apoptosis
High entropy
Low entropy

Figure 6 Possible scenarios explaining the decline of fetal cortical entropy with *in utero* maturation. (A) Cortical entropy may decline with gestational age in fetuses due to maturation of auditory evoked responses to auditory tones, which should impose structure on the cortical signal, thus minimizing its entropy. This scenario explains decreases in entropy driven event related fields (ERFs), yet leaves non-ERF driven changes unexplained. Our finding of decreasing cortical entropy with maturation persisted even after subtracting cortical response templates (CRTs) that model the auditory ERF; thus, the decline in entropy appears to be partly or mostly non-ERF driven. (B) Our finding of declining entropy may also be puzzling because it excludes the spatial dimension of the cortical response, which is needed to relate perturbational complexity to consciousness in adults. It is possible that while temporal cortical entropy decreases with gestational age in fetuses, a greater change in spatial cortical entropy occurs in the opposite direction (i.e., increasing). (C) Alternatively, our results might be understood in the context of the entropic brain hypothesis (EBH), which predicts that over-entropic levels existing above a global optimum for consciousness (i.e., a critical point) should be related to declining levels of consciousness; thus, decreases in entropy toward this critical point should correspond to increases in the conscious level. However, we did not find greater evidence of noise (i.e., stochasticity) in younger fetuses, thus casting doubt on this explanation. In the diagram illustrated here, vertical axis correspond to entropy level and the pink curve corresponds to the level of consciousness, with the green highlighted region representing the critical zone that is optimal for consciousness. (D) Finally, the maturational decline in fetal entropy might be unrelated to consciousness. Instead, it could reflect developmental processes such as apoptosis and synaptic pruning that reduce the number of ways in which neural circuits can be arranged (i.e., entropy). In this illustration, multiple circuit configurations (left) are possibly prior to the canalization process which brings circuits toward a genetically determined phenotype (right).

Tables

Sample	Measure	Maturation t-stat	Maturation P_{FDR}	HRV t-stat	HRV P_{FDR}
Fetal	CTW	-3.50	**0.00188**	-2.01	0.0992
Fetal	LZC	-3.64	**0.00177**	-1.96	0.107
Fetal	PermEn32	-4.71	**6.87E-05**	-0.189	0.957
Fetal	PermEn64	-2.57	**0.0325**	0.135	0.98
Fetal	mMSE	-3.16	**0.00583**	-1.63	0.182
Fetal	mSampEn	-3.81	**0.00177**	-1.77	0.146
Newborn	CTW	-2.45	**0.0476**	0.747	0.605
Newborn	LZC	-2.23	0.0726	0.685	0.644
Newborn	PermEn32	-3.85	**0.00177**	2.38	0.0544
Newborn	PermEn64	-1.61	0.19	1.17	0.37
Newborn	mMSE	-2.15	0.0853	0.813	0.577
Newborn	mSampEn	-2.72	**0.0263**	1.06	0.421

Table 1 Predictors of cortical entropy in fetuses and newborns. All entropy measures were significantly predicted by gestational age in fetuses and one out of six entropy measures were significantly predicted by age in newborns. Note that PermEn32 (sensitive to 4 – 10 Hz activity) strongly related to maturation in both fetuses and newborns ($p < 0.005$), whereas PermEn64 (sensitive to 2 – 5 Hz activity) did not relate to maturation in newborns, and its relationship with maturation in fetuses was only marginally significant ($p = 0.03$), suggesting that maturation relates strongly to MEG entropy in the perinatal alpha band. No entropy measures were significantly predicted by HRV—used as a proxy for arousal—in either cohort (note, however, a trend toward greater PermEn32 with greater HRV in newborns, $p = 0.05$).

Cohort	Entropy measure	t-stat	P_{FDR}
Fetal	CTW	0.835	0.577
Fetal	LZC	0.385	0.854
Fetal	PermEn32	43.7	**2.86E-12**
Fetal	PermEn64	33	**4.61E-11**
Fetal	mMSE	1.6	0.22
Fetal	mSampEn	1.32	0.325
Neonatal	CTW	0.557	0.746
Neonatal	LZC	0.631	0.698
Neonatal	PermEn32	115	**1.46E-12**
Neonatal	PermEn64	129	**1.12E-12**
Neonatal	mMSE	0.279	0.931
Neonatal	mSampEn	0.107	1.00

Table 2 Differences between amplitude and non-amplitude (phase + amplitude x phase interaction) components of entropy changes in fetuses and newborns. In both fetal and neonatal data, the amplitude component drives decreases in PermEn with maturation, whereas the non-amplitude component drives decreases in in PermEn with maturation (true for both τ = 32 ms and τ = 64 ms). Neonatal results in the above table are referenced to younger subjects; for results referened to older subjects, see Table SX.

Sample	Measure	t-stat	P_{FDR}
Fetuses	CTW	-1.70	0.164
Fetuses	LZC	-1.58	0.190
Fetuses	PermEnE32	-2.05	0.0942
Fetuses	PermEn64	-0.224	0.958
Fetuses	mMSE	-0.76	0.602
Fetuses	mSampEn	1.85	0.131
Newborns	CTW	-1.00	0.452
Newborns	LZC	-0.450	0.809
Newborns	PermEn32	-4.05E-15	1.00
Newborns	PermEn64	2.93E-14	1.00
Newborns	mMSE	-0.0716	1.00
Newborns	mSampEn	2.56	**0.0339**

Table 3 Surrogate data testing of MEG complexity measures in fetuses and newborns. Entropy measures computed from cortical signals were compared to the median entropy across 100 surrogate signals. Significant differences between entropy from cortical and surrogates signals were assessed using linear mixed models (LMMs). Bolded p-values are significant; surrogacy only significantly predicted entropy using mSampEn in newborns (p = 0.034).

Sample	Predictor	Direction	P_{FDR}	Estimated	Cluster size	Cluster intensity	Minimum frequency	Maximum frequency	Minimum time	Maximum time
Fetuses	GA	Positive	**0.00177**	Yes	178	564.52	1.45	1.87	2563.6	2854.5
Fetuses	GA	Positive	**0.00177**	Yes	150	470.19	1.09	1.37	36.4	236.4
Fetuses	GA	Positive	**0.00177**	Yes	128	408.57	2.54	3.08	1672.7	1981.8
Fetuses	GA	Positive	0.0598	No	20	60.39	1.70	1.83	1381.8	1454.5
Fetuses	GA	Positive	0.0863	No	14	42.69	1.48	1.70	90.9	90.9
Fetuses	GA	Positive	0.142	No	9	25.63	2.38	2.59	963.6	963.6
Fetuses	GA	Positive	0.142	No	9	26.42	1.30	1.38	2836.4	2854.5
Fetuses	GA	Positive	1.00	No	2	5.68	1.68	1.68	1254.5	1272.7
Fetuses	GA	Negative	1.00	No	2	5.69	7.34	7.42	236.4	236.4
Fetuses	GA	Negative	1.00	No	1	2.84	8.72	8.72	1254.5	1254.5
Newborns	Age	Positive	**0.00177**	Yes	1272	4591.34	2.33	11.56	1818.2	2563.6
Newborns	Age	Positive	**0.00177**	Yes	1215	4411.54	1.00	1.79	-200.0	1218.2
Newborns	Age	Positive	**0.00177**	Yes	903	3354.37	3.22	13.45	381.8	1109.1
Newborns	Age	Positive	**0.00177**	Yes	628	2211.70	1.68	5.66	-200.0	109.1
Newborns	Age	Positive	**0.00177**	Yes	161	538.72	1.04	1.41	2400.0	3000.0
Newborns	Age	Positive	**0.00177**	Yes	114	356.74	3.22	4.76	2854.5	3000.0
Newborns	Age	Positive	**0.00177**	Yes	49	150.06	1.38	1.72	1418.2	1563.6
Newborns	Age	Positive	**0.00177**	Yes	43	127.26	3.29	3.67	218.2	381.8
Newborns	Age	Positive	0.0969	No	14	55.34	1.00	1.00	1981.8	2218.2
Newborns	Age	Positive	0.181	No	9	27.89	13.45	13.45	-200.0	-54.5
Newborns	Age	Positive	0.205	No	8	24.96	11.56	13.45	672.7	672.7
Newborns	SDNN	Negative	**0.00177**	Yes	142	479.38	4.00	6.73	1818.2	2000.0
Newborns	SDNN	Negative	**0.00177**	Yes	138	472.52	2.59	3.36	-36.4	436.4
Newborns	SDNN	Negative	**0.00177**	Yes	73	224.33	2.65	3.36	1254.5	1563.6
Newborns	SDNN	Negative	0.131	No	11	36.71	1.00	1.00	1981.8	2163.6
Newborns	SDNN	Negative	1.00	No	2	6.02	1.00	1.00	2545.5	2563.6

Table 4 Time-frequency clusters in fetuses and newborns. Statistically significant p-values are bolded. The 'Estimated' column reports whether the cluster was greater in size than all 2000 permutations; in these cases, we used 1/(Nperm+1) to derive the p-value prior to an FDR correction, where Nperm is the number of permutations (2000). Note that p-values were estimated for all significant clusters. In total, we report three significant clusters for which gestational age (GA) is significantly predictive of spectral power in fetuses (positive relationship), eight clusters for which age is significantly predictive of spectral power in newborns (positive relationship), and three clusters for which arousal (SDNN) is significantly predictive of spectral power in newborns (negative relationship). Note that minimum/maximum frequency/time do not delineate the points at which the effect beings and ends, i.e., cluster boundaries contain the effect within a certain degree of confidence cannot give information concerning its exact onset or offset along the frequency or time dimension.